Quasicoherent Oscillations Induced by Nonthermal Electrons during Magnetic Reconnection in the T-10 Tokamak

P.V. Savrukhin* and V.V. Volkov

Nuclear Fusion Institute, RRC "Kurchatov Institute," 123182, Moscow, Russia

(Received 19 March 2003; published 3 March 2004)

Small-scale quasicoherent oscillations of the x-ray emissivity and magnetic field perturbations are observed in the T-10 tokamak during abrupt growth of the $m = 2$, $n = 1$ magnetohydrodynamic modes at the density limit disruption. Analysis indicates a possible link between the small-scale oscillations and nonthermal electron beams induced around the X points of the $m = 2$, $n = 1$ magnetic island during reconnection of magnetic field lines at the disruption instability.

DOI: 10.1103/PhysRevLett.92.095002 PACS numbers: 52.55.Fa, 52.35.Py, 52.35.Vd, 52.70.La

Acceleration of electrons to suprathermal energies, $E_\gamma \sim 100$ keV, is a typical feature of magnetic reconnection in a variety of plasma phenomena ranging from large-scale astrophysics events (e.g., solar flares) to energy relaxations and disruptions in laboratory experiments [1,2]. The effect can be especially important during the disruption instability in high-temperature collisionless plasma in tokamaks, when electron acceleration represents one of the dominant mechanisms of current dissipation in the reconnection layer [3,4]. Experimental analysis has in fact revealed the generation of localized beams of the suprathermal electrons around the X points of the $m = 1$, $n = 1$ and $m = 2$, $n = 1$ magnetic islands during internal and major disruptions in tokamak [5] (here, n, m are longitudinal and transverse wave numbers). However, details of the process are still not clear at the moment. The particular problem of the beam dynamics is connected with instabilities possibly induced by the fast electrons in a magnetized plasma [6].

A classical instability of high-energy electrons is connected with the movement of the beams through magnetic fields with periodic structure [6,7]. Periodic modulation of the magnetic fields in tokamaks can be connected, for example, with a variety of stray fields, arising from imperfect alignment of a tokamak magnetic system. In particular, strong field modulation can be produced by the magnetic ripples due to a discrete number of the toroidal field coils [see Fig. 1(a)]. Movement of the electrons through the magnetic ripples leads to modulation of the beams and can be accompanied by an induced radiation.

In this Letter, we identify and analyze small-scale quasicoherent oscillations of the x-ray intensity and perturbations of magnetic fields accompanying large-scale MHD modes during disruptions at high density in the T-10 tokamak (minor and major radii, $a = 0.3m$, $R_0 = 1.5m$, respectively). While a variety of phenomenologically similar small-scale perturbations were observed during the abrupt growth of MHD modes in previous tokamak experiments [see, for example, ballooning modes ($n \sim 10$) [8], microtearing modes ($m \sim 7$–20) [9], or high-harmonic secondary oscillations induced due to nonlinear mode coupling [10]], present experiments suggest a new type of instability possibly connected with nonthermal electron beams localized around the magnetic islands.

One of the key elements of the present experiments is connected with measurements of the x-ray radiation in a direction tangential to the helical field lines using toroidally viewing x-ray array [see *TX* array - 4, in Fig. 1] [11]. The *TX* array consists of three Si and CdTe detectors with an adjustable field of view covering in subsequent discharges the plasma area $0.3 < r/a < 0.9$ (spatial resolution of the systems is $dr = 0.7$ cm, data acquisition frequency is up to $F_A = 330$ kHz, energy range $E_\gamma =$ 2–150 keV). The array provides superior resolution of the small-scale helical perturbations and allows the identification of the localized fluctuations of nonthermal x-ray emission, not analyzed previously in detail in tokamaks due to limited spatial and time resolution of the diagnostics [12]. The x-ray intensity in the direction orthogonal to the plasma column is measured by the standard Si diodes *XRA* (5), *XRB* (6), *XRC* (7) (up to 58 channels), and multiwire gas detector *XWD* (8) (up to 32 channels).

Experimental results.—Fig. 2 shows a typical time evolution of the plasma parameters observed during

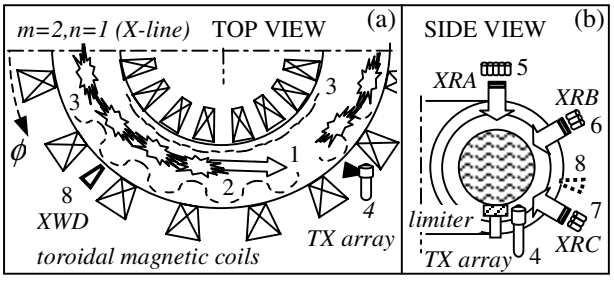

FIG. 1. Schematic view of the magnetic system and diagnostics in the T-10 tokamak. Quasicoherent nonthermal x-ray radiation (1) is generated by electron beams (2) moving through the magnetic field with ripples (3).

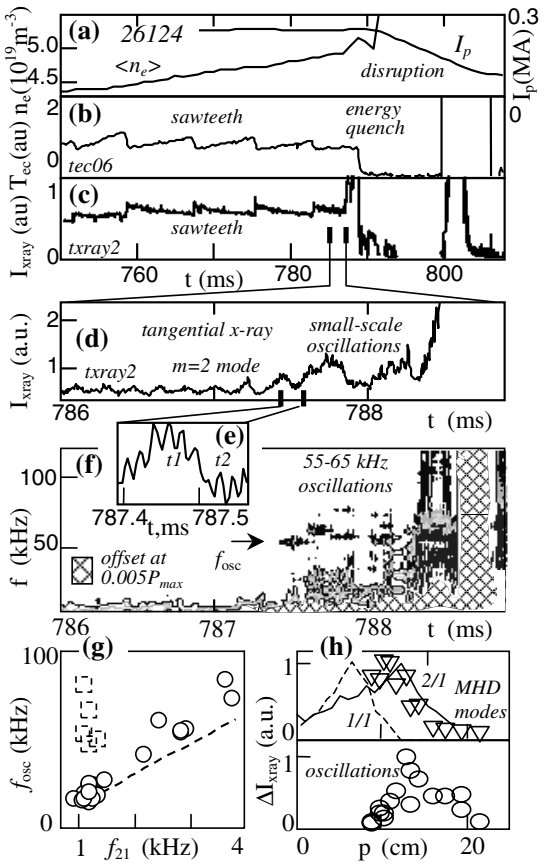

FIG. 2. (a),(b) Time evolution of the central line-averaged electron density $\langle n_e \rangle$, plasma current, I_p, and ECE emission, T_{ec}, prior the density limit disruption. Time evolution (c)–(e) and spectrogram (f) of the x-ray intensity measured with the tangential x-ray array. (g) Repetition rate of the dominant (circles) and secondary (dashed rectangles) harmonics of the small-scale x-ray oscillations in plasma discharges with various frequency of the $m = 2$, $n = 1$ mode rotation, f_{21}. The dashed line represents the dependence $f_{osc} \sim 16 f_{21}$. (h) Radial profiles of amplitude of the small-scale x-ray oscillations (circles) and MHD modes (triangles) measured using the *TX* array. Dashed and solid lines represent the amplitude of the singular $m = 1$, $n = 1$ mode (sawtooth precursor) and coupled $m = 1$ and $m = 2$ modes, respectively, measured by the gas detector *XWD*.

density limit disruption in deuterium plasma with toroidal field $B_t = 2.4$ T, and a moderate level of rf power, $P_{ec} = 0.25$ MW. Similar to previous experiments, energy quench ($t \sim 788.5$ ms) is preceded by the growth of large-scale $m = 2$, $n = 1$ helical perturbations coupled with the $m = 1$, $n = 1$ modes in the plasma core. Large-scale MHD modes are additionally superimposed with small-scale oscillations observed most clearly with the tangentially viewing x-ray array [see Figs. 2(d) and 2(e)]. The small-scale oscillations are localized around the $m = 2$, $n = 1$ modes [see Fig. 2(h)] and are typically represented by a solitary harmonic in the perturbation spectrum [see the quasicoherent spikes at frequency $f \sim$ 55–65 kHz ($t < 788$ ms) in Fig. 2(f)]. In some cases, additional oscillations with extremely small amplitude are also observed at higher frequencies [see rectangles in Fig. 2(g)]. These high frequency oscillations are not well resolved with the present diagnostic technique and are not studied here in detail. The repetition rate of the dominant harmonic is changed considerably in various plasma conditions ($f_{osc} \sim$ 15–85 kHz); however no clear dependence of the oscillation frequency on the plasma parameters was found so far in the experiments [$\langle n_e \rangle = (2.5\text{–}6)10^{19}$ m^{-3}, $I_p = 0.09$–0.35 MA, $B_t = 2.0$–2.5 T]. Meanwhile, experiments indicate a direct connection of the repetition rate with rotation of the $m = 2$ mode [Fig. 2(g)].

Small-scale oscillations of the x-ray intensity are accompanied by perturbations of the poloidal magnetic field measured by magnetic probes [9] placed inside the vacuum vessel close to the plasma boundary (Fig. 3). Analysis of phase shifts of the magnetic perturbations identified using five magnetic probes with narrow poloidal separation ($dl_\theta = 3$ cm) indicates a modelike structure of the oscillations traveling in the same direction as one of the $m = 2$, $n = 1$ MHD modes (compare dashed lines in Fig. 3 at time moments $t3$, $t4$ and $t1$, $t2$, for the small-scale oscillations and the $m = 2$ mode, accordingly). However, sometimes phase shifts of the magnetic perturbations can be changed in subsequent cycles (see marks $t5$–$t6$), indicating transition from the "modelike" to a "shock" structure of the oscillations.

Small-scale oscillations are often transformed to intensive x-ray bursts with maximum amplitude at the growing phase and at the top of the $m = 2$, $n = 1$ perturbations. Amplitudes of the bursts are modulated in this case with the same frequency as one of the quasicoherent oscillations [5,13].

Discussion.—Several possible mechanisms can be used for the explanation of the small-scale oscillations. Connection of the oscillations with localization of the MHD mode is phenomenologically similar to the

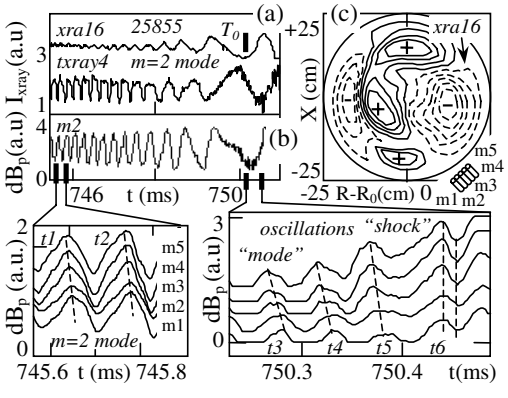

FIG. 3. (a),(b) Time evolution of the x-ray intensity, $I_{x\ ray}$, and poloidal magnetic field perturbations, dB_p, prior to the density limit disruption ($t \sim 750.7$ ms). (c) Tomographically reconstructed image of the x-ray perturbations measured by conventional x-ray detectors at time $T_0 = 750.096$ ms.

phenomena of ballooning modes observed in previous experiments [8]. However, the relatively low magnetohydrodynamic pressure in present studies ($\beta_p \sim 0.05$) and the continuous growth of the oscillations in respect to various phases of the $m = 2$ mode [see similar amplitudes of the oscillations at time moments $t1$, $t2$ in Fig. 2(e)] seem to exclude a possible ballooning origin of the perturbations. Furthermore, the relatively narrow spectrum of the oscillations observed in the experiments is in sharp contrast with the broadband perturbations typically induced during the energy quench [compare $t \sim$ 787.5 ms and $t > 788.3$ ms in Fig. 2(f) accordingly]. This effect as well as the shocklike magnetic perturbations with no poloidal phase shifts contradicts a possible connection of the oscillations with high-m, n tearing modes [9,10]. Furthermore, weak dependence of the repetition rate $f_{\rm osc}$ on plasma parameters (n_e, B_t) can also indicate no connection of the oscillations with an instability of fast ions (e.g., *TAE* modes [14]).

Enhanced amplitude of the small-scale oscillations identified with the tangentially viewing x-ray array in comparison with the standard x-ray measurements in orthogonal direction indicates a possible connection of the phenomena with beams of fast electrons localized around the X points (X line) of the $m = 2$, $n = 1$ magnetic island [5,13]. While the experimental data are not sufficient to produce a comprehensive model for the cause of the observed oscillations, the phenomena could possibly be described by the following simplified process. Appearance of nonthermal electrons around a magnetic island is naturally expected in the presence of strong electric fields during magnetic reconnection. Acceleration of electrons in the electric fields is balanced initially by drag associated with Coulomb collisions. The collision frequency decreases with increasing electron velocity. This implies that above a critical electric field electrons gain a longitudinal velocity high enough to be continuously accelerated (''runaway'' [14]). The mechanism of the runaway generation is important in the region of strong induced electric fields around the X points (line) of the magnetic island, while outside the reconnection layer (in plasma regions with only low equilibrium electric field) the nonthermal electrons are effectively slowing down due to collisions with the background plasma. The process of generation and loss of the electrons can therefore lead to formation of a helical nonthermal beam with maximum density around the X line of the magnetic island. Rotation of the $m = 2$, $n = 1$ modes introduces two typical motions of the nonthermal electrons: continuous acceleration in a longitudinal direction along the helical X line (typical electron velocity is up to $v_r/c \sim$ 0.5 in the case) and driftlike motion of the beams with angular velocity of the order of $v_{II} \sim R_0\omega_m$, where ω_m is the frequency of the mode rotation [Fig. 4(a)]. A nonthermal beam moving in a magnetized plasma through a perturbed magnetic field (here, equilibrium magnetic field with ripples) is a potential source of induced

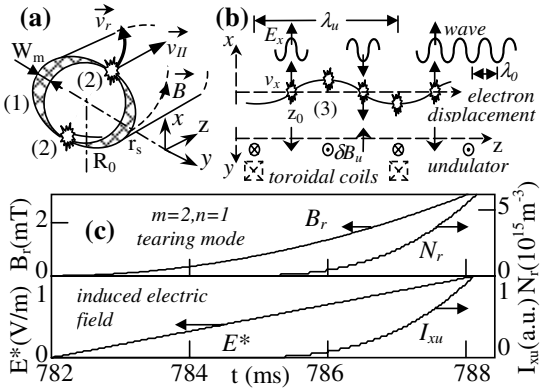

FIG. 4. (a) Schematic view of the $m = 2$ magnetic islands (1) with beams of the nonthermal electrons (2). (b) Resonant interaction of an oscillating electron (3) with a transverse electromagnetic wave, E_x. The electron is shown at five different times while it traverses an undulator period of length λ_u. At the ''injection'' point (z_0) the undulator magnetic field deflects the electron in the transverse direction, against the force exerted by the wave electric field. As a result the electron energy is transferred to the wave. Initial phase and frequency of the wave are chosen such that the electron loses energy over the whole undulator period. Rectangles indicate, schematically, the positions of tokamak toroidal field coils. (c) Calculated amplitude of the magnetic field perturbations (B_r), density of the nonthermal electrons (N_r), electric field generated during reconnection (E^*), and amplitude of the induced x-ray radiation (I_{xu}).

radiation [6,7]. A possible mechanism of resonant transfer of electron kinetic energy to a transverse electromagnetic wave is represented schematically in the case in Fig. 4(b). (A plane-wave electric field interacting with a single electron is considered here for simplicity [15].) Nonthermal electron moving in respect to a perturbed magnetic field experiences periodic displacement in a transverse direction. If an external wave with an electric field vector E_x copropagating with an electron counteracts the transverse oscillatory motion of the electron, the energy can be transferred from the electron and the wave is amplified. This occurs on resonances when the electron slips behind the external wave by one wavelength, λ_0, while the electron transverses the undulator period, λ_u. The resonance condition can be written in this case as $(\lambda_0 + \lambda_u)/c = \lambda_u(1 + a_w^2/4\gamma^2)/v_{II}$, where v_{II} is the average longitudinal electron velocity, γ is the relativistic factor, $\gamma = [1 - (v_{II}/c)^2]^{-1/2}$, a_w is an undulator parameter, $a_w = e\lambda_u\delta B/(2\pi mc)$, and δB is the amplitude of the perturbed magnetic field. Energy modulation during the longitudinal motion also causes the electron to bunch with a period of an ''external'' wavelength. At resonance the bunching occurs at a phase of the field where there is no net exchange of energy. Modulation of the electron density inside the helical beam leads to oscillations of the x-ray emissivity, which can be measured in experiments. For a typical beam energy, $E_b \sim$ 80–100 keV, movement of electrons along the X line can

be accompanied by radiation in a frequency range of the order of 100 MHz; however the intensity of such radiation is extremely small due to low density and nonmonochromatic energy distribution of the beams. Measurements of such oscillations are outside the capabilities of the present diagnostic techniques. Driftlike motion connected with rotation of the mode can be accompanied by an induced radiation in a frequency range $\Omega_u \sim 2\pi v_{II}/(\epsilon_u \lambda_u)$, which is of the order of 20–70 kHz for typical parameters in a T-10 tokamak (here $\epsilon_u \sim 1$ is a numerical parameter representing bending of the beam trajectory, $\epsilon_u \sim 1 + a_w^2/4$). While calculations indicate in the case up to 30% lower values of the oscillations frequency [see dashed line in Fig. 2(g)] than one measured in the experiments, the mechanism could probably justify a link between the oscillations and the rotation of the $m = 2$ mode, similar to the one observed in experiments.

Results of calculations for typical conditions of the experiments in T-10 are shown in Fig. 4. Growth of MHD perturbations is described by the tearing mode equation [16]: $dW_m/dt = 1.2(\eta/\mu_0)\Delta'_m$, where, Δ'_m is the stability parameter, η is the plasma resistivity, dW_m is the width of the magnetic island, $dW_m = 4(B_r r_s R_0/nsB_t)^{1/2}$, r_s is the radius of the magnetic surface, B_r is the radial magnetic field perturbations, and s is the magnetic shear. (For simplicity, effects of the "neoclassical" bootstrap currents and ion polarization flows are not considered in the present analysis of T-10 experiments with low magnetohydrodynamic pressure.) Growth of the tearing mode is accompanied by the generation of induced electric fields [3]: $E^* \sim (sB_t/16r_s)W_m dW_m/dt$, with subsequent formation of the nonthermal electron beam with density, N_r. In a simplified way, the time evolution of the density of runaway electrons (N_r) generated by applied electric fields in a thermal plasma with density n_e can be described by the equation [14]:

$$\partial N_r/\partial t + \nabla \cdot (\mathbf{v}_r N_r) = n_e/\tau_{\rm dr} + N_r/\tau_{\rm av} - \nabla \boldsymbol{\Gamma}_{\rm loss},$$

where $|\mathbf{v}_r| \sim 0.5c$ is the runaway electron mean velocity, $1/\tau_{\rm dr}$ and $1/\tau_{\rm av}$ are the production rates of the primary runaway electrons (Dreicer acceleration) and secondary knock-on avalanche, accordingly, and flux $\boldsymbol{\Gamma}_{\rm loss}$ denotes losses of the nonthermal electrons. (Analysis [5,13] indicated that Dreicer acceleration is the dominant mechanism of the runaway generation inside the reconnection layer.) Radiated power induced by the beams depends on the product $E_x v_x$ averaged over the undulator period. In a simplified way, the amplitude of induced oscillations is determined by the relation [15] $I_{xu} \sim c_1(eE_{x0}v_{II}a_w)N_r V_{\rm vol}$, where $E_{x0} \sim r_s \omega_m \delta B/\lambda_u$, $V_{\rm vol} \sim (m/n)W_m r_s R_0$, and c_1 is a normalizing factor. Similar to the experimental observations, calculations indicate explosive growth of induced oscillations, I_{xu}, with a time delay with respect to the MHD perturbations.

It should be pointed out, however, that in spite of qualitative agreement with experiments, present calculations use an oversimplified model of monoenergetic nonthermal beams interacting with the straight undulator. Detailed calculations of the wave-beam interaction are required for analysis of the induced oscillations in real experimental conditions. Meanwhile, connection of the oscillations with localized beams of the nonthermal electrons analyzed in present experiments can possibly represent a general phenomenon accompanying disruptions in tokamaks, not resolved previously due to diagnostic limitations. This is confirmed indirectly by previously reported observations that nonthermal electron cyclotron emission often precedes disruptions at high β [8]. The x-ray perturbations peak in this case at smaller tangency radius than the local electron cyclotron emission (ECE) fluctuations, which indicates that relativistically downshifted emission in the presence of the nonthermal electron beams ($E_\gamma \sim 100$ keV) could also be responsible in part for the ballooninglike perturbations in high β plasmas [8].

The authors would like to thank A.V. Sushkov for providing gas detector data, and S.V. Mirnov, F. Porcelli, K. A. Razumova, I. B. Semenov, and V. A. Vershkov for stimulating discussions. This work was supported in part by RFBR 01-02-16768 and INFM FOES000754-OA03000130.

*Present address: Burning Plasma Research Group, INFM, and Department of Energetics, Politecnico di Torino, 10129, Italy.

[1] D. Biskamp, *Magnetic Reconnection in Plasmas* (Cambridge University Press, Cambridge, 2000).
[2] S. I. Syrovatskii, Astron. Zh. (Sov. Astron.) **43**, 340 (1966).
[3] J. A. Wesson, Nucl. Fusion **30**, 2545 (1990).
[4] F. Porcelli *et al.*, Plasma Phys. Controlled Fusion **44**, B389 (2002).
[5] P.V. Savrukhin, Phys. Rev. Lett. **86**, 3036 (2001).
[6] R. C. Davidson, *Theory of Nonneutral Plasmas* (Imperial College Press, London, 2001).
[7] V. L. Ginzburg, Izv. Akad. Nauk SSSR, Ser. Fiz. **11**, 165 (1947).
[8] E. P. Fredrickson *et al.*, Phys. Plasmas **2**, 4216 (1995).
[9] V.V. Volkov *et al.*, Sov. J. Plasma Phys. **16**, 295 (1990).
[10] A. Bondeson *et al.*, Nucl. Fusion **31**, 1695 (1991).
[11] P.V. Savrukhin and I.V. Klimanov, Rev. Sci. Instrum. **72**, 1668 (2001).
[12] S. VonGoeler *et al.*, Nucl. Fusion **25**, 1515 (1985).
[13] P.V. Savrukhin, Phys. Plasmas **9**, 3421 (2002).
[14] ITER Physics Expert Group on Disruptions, Plasma Control, and MHD, ITER Physics Basis Editors, Nucl. Fusion **39**, 2251 (1999).
[15] S. Humphries, Jr., *Charged Particle Beams* (John Wiley and Sons, New York, 1990).
[16] G. Bateman, *MHD Instability* (The MIT Press, Cambridge, 1979).